International Journal of High-Rise Buildings
June 2014, Vol 3, No 2, 121-145

International Journal of
High-Rise Buildings
www.ctbuh-korea.org/ijhrb/index.php

A Study on Optimum Distribution of Story Shear Force Coefficient for Seismic Design of Multi-story Structure

Sang Hoon Oh and Jongsoo Jeon†

Department of Architectural Engineering, Pusan National University, Korea

Abstract

The story shear force distributions of most seismic design codes generally reflect the influences of higher vibration modes based on the elastic deformations of structures. However, as the seismic design allows for the plastic behavior of a structure, the story shear force distribution shall be effective after it is yielded due to earthquake excitation. Hence this study conducted numerical analyses on the story shear force distributions of most seismic design codes to find out the characteristics of how a structure is damaged between stories. Analysis results show that the more forces are distributed onto high stories, the lower its concentration is and the more energy is absorbed. From the results, this study proposes the optimum story shear force distribution and its calculation formula that make the damages uniformly distributed onto whole stories. Consequently, the story damage distribution from the optimum calculation formula was considerably more stable than existing seismic design codes.

Keywords: Optimum distribution of story shear force coefficient, Accumulative plastic deformation ratio

1. Introduction

Typically, the story shear force acting horizontally on a multi-story structure is proportionally calculated to the height of and weight acting upon each story. However, if dynamic load such as earthquake is acting on it, this rule does not apply to the distributed load acting upon every story under the influence of higher vibration modes. For this reason, seismic design code of several countries around the world analyze the characteristics of load distribution caused by higher vibration modes in various ways and provide various forms of the modification factor of the story shear force distribution accordingly.

Most of the seismic design code around the world use the analysis method based on Elastic Strain Range such as Response Spectrum Analysis Method and Mode Superposition Method in order to analyze the effects of higher vibration modes. Since the plastic deformation is allowed in seismic design in some degree up to the collapse of building, the needs for securing the enough stability arise in consideration of elastic deformation as well as the behaviors after the occurrence of plastic deformation in analyzing the seismic load.

By conducting the static and dynamic response analyses based on the calculation formula for the story shear force distribution, which is proposed by the seismic design code of several countries, in this paper we weigh the behaviors of a multi-story structure including plastic deformation, and analyze the characteristics of damage distribution caused by vibratory ground motion. Based on these results, the point of this paper is to propose the optimized calculation formula for the story shear force distribution in order to improve the seismic performance by distributing the seismic load evenly on all stories.

†Corresponding author: Jongsoo Jeon
Tel: +82-51-510-7608; Fax: +82-51-514-2230
E-mail: js1842@nate.com

2. Comparisons of Story Shear Force Distribution of Seismic Design Code around the World

This study adopted the criteria for seismic design codes shown in Table 2-1.

2.1. Calculation formula for the story shear force distribution

The design procedure of the story shear force by the equivalent static analysis method comprises two parts: calculating the base shear, occurring on the lowest part of a structure by seismic load and calculating the story shear force by distributing the seismic load to all stories. The

Table 2-1. The seismic design code of several countries used for this study

Seismic design code	Proposed Country	Proposed Year
KBC2009[3]	Republic of Korea	2009
IBC2006[4]	USA(Integrated)	2006
UBC97[5]	USA(West)	1997
AIJ[6]	Japan (Architectural Institute of Japan : AIJ)	1981
NZS1170[7]	New Zealand	2003

story shear force distribution is determined during the distribution process of seismic load, and the seismic design code of several countries propose the story shear force distribution considering the effects of higher vibration modes by applying the modification coefficient during this process. The base shear calculation formula and the seismic load distribution formula, used in this study and proposed by the seismic design code, are as shown in Table 2-2 and 2-3 respectively.

2.2. Comparing and weighing the story shear force distribution

Examining the story shear force calculation formula of the seismic design code around the world reveals that the base shear calculation formula and the seismic load distribution formula are not in constant manner, which in turn affect the size and distribution type of the story shear force in various forms. For this reason, we specify structure models, as shown in Table 2-4, calculate the story shear force based on each seismic design code, and com-

Table 2-2. Base shear calculation formula of the seismic design code

Category	Base shear calculation formula
KBC2009	$\min\{V=\frac{S_{D1}}{\left(\frac{R}{I_E}\right)T}\cdot W,\quad V=\frac{S_{DS}}{\left(\frac{R}{I_E}\right)}\cdot W\}$ V=0.01 or more
IBC2006	$\min\{V=\frac{S_{D1}}{\left(\frac{R}{I_E}\right)T}\cdot W,\quad V=\frac{S_{D1}T_L}{\left(\frac{R}{I_E}\right)T^2}\cdot W\}$ (T>T_L) $\min\{V=\frac{S_{D1}}{\left(\frac{R}{I_E}\right)T}\cdot W,\quad V=\frac{S_{DS}}{\left(\frac{R}{I_E}\right)}\cdot W\}$ (T≤T_L) V=0.01 or more
UBC97	$V=\frac{C_v I}{RT}W,\ V_{max}=\frac{2.5Cal}{R}W,\ V_{min}=0.11CalW$
NZS1170	$V=C_h(T_1,u)S_pRZL_uW_t$
AIJ	$Q_i=ZR_tA_iC_o\Sigma W_i$

Table 2-3. Lateral story forces of the seismic design code

Category	Lateral story forces distribution formula	Reflection methods of higher vibration modes
KBC2009	$F_x=\frac{W_x h_x^k}{\Sigma_{i=1}^n W_i h_i^k}\cdot V$	Applying the distribution factor according to the period of structure
IBC2006	$F_x=\frac{W_x h_x^k}{\Sigma_{i=1}^n W_i h_i^k}\cdot V$	
UBC97	$F_x=\frac{(V-F_t)W_x h_x}{\Sigma_{i=1}^n W_i h_i}$	Applying the horizontal force acting on roof story
NZS1170	$F_x=F_t+0.92V\frac{W_x h_x}{\Sigma_{i=1}^n W_i h_i}$	Applying the horizontal load acting on roof story
AIJ	$A_i=1+\left(\frac{1}{\sqrt{\alpha_i}}-\alpha_i\right)\times\frac{2T}{1+3T},\ \left(\alpha_i=\Sigma\frac{W_i}{W_T}\right)$	story shear force distribution factor according to vertical valid weight ratio

Table 2-4. Structural conditions for calculating the story shear force distributions

Category	Structural design requirements
Use	General Office Building
Structure Classification	Steel ordinary moment frames
Shape	Plane (width × height) = 8m × 8m / story height = 3m
Weight	(Sum of general dead load and live load :)
Area & Ground characteristics	Using the most dominant region and modulus subgrade reaction in each standard
Stories(Aspect Ratio)	3-story (1.125), 5-story (1.875), 10-story (3.75), 20-story (7.5)

pare the distributions in this study.

The above requirements were applied to the story shear force distribution calculation formula (Table 2-2, 2-3) based on each seismic design code. The calculation results are as shown in Fig. 2-1. Since the modulus subgrade reaction is differently applied for each region, the size of base shear calculated for each seismic design code is different from each other. With this in mind, based on the result value of story shear force from Fig. 2-1, the story shear force distribution of each story, normalized by the size of the base shear force, is shown in Fig. 2-2, and the distribution types are compared accordingly.

However, as shown in the graph, this type of expression does not sufficiently display the differences of the distribution values based on each seismic design code, so it is not appropriate to compare the story shear force distributions. The next section introduces the concept on distribution of yield story shear force coefficients which describes the layer strength distribution of a structure, and weighs the story shear force distribution based on each seismic design code by using the distribution of yield story shear force coefficients.

2.2.1. Distribution of yield story shear force coefficients

The "Seismic design of a structure according to Energy Balance Method2)" proposes the concept of yield story shear force coefficient, which indicates the strength for the load acting on each story, in order to control and evaluate the layer damage. The yield story shear force of each story Q_{yi} divided by the weight of the upper structure equals the yield story shear force coefficient α_i, as shown in Formula (2.5):

$$\alpha_i = \frac{Q_{yi}}{\Sigma_{j=i}^{N} W_j} \tag{2.5}$$

when, Q_{yi} : Yield story shear force on the i story
$\Sigma_{j=i}^{N} W_j$: Total weight on i story of upper structure

The distribution of yield story shear force coefficient $\overline{\alpha_i}$ refers to the ratio of the yield shear force coefficient on each story to the 1st story, as shown in Formula (2.6):

$$\overline{\alpha_i} = \alpha_i / \alpha_1 \tag{2.6}$$

when, $\overline{\alpha_i}$: Yield shear force coefficient at the i story

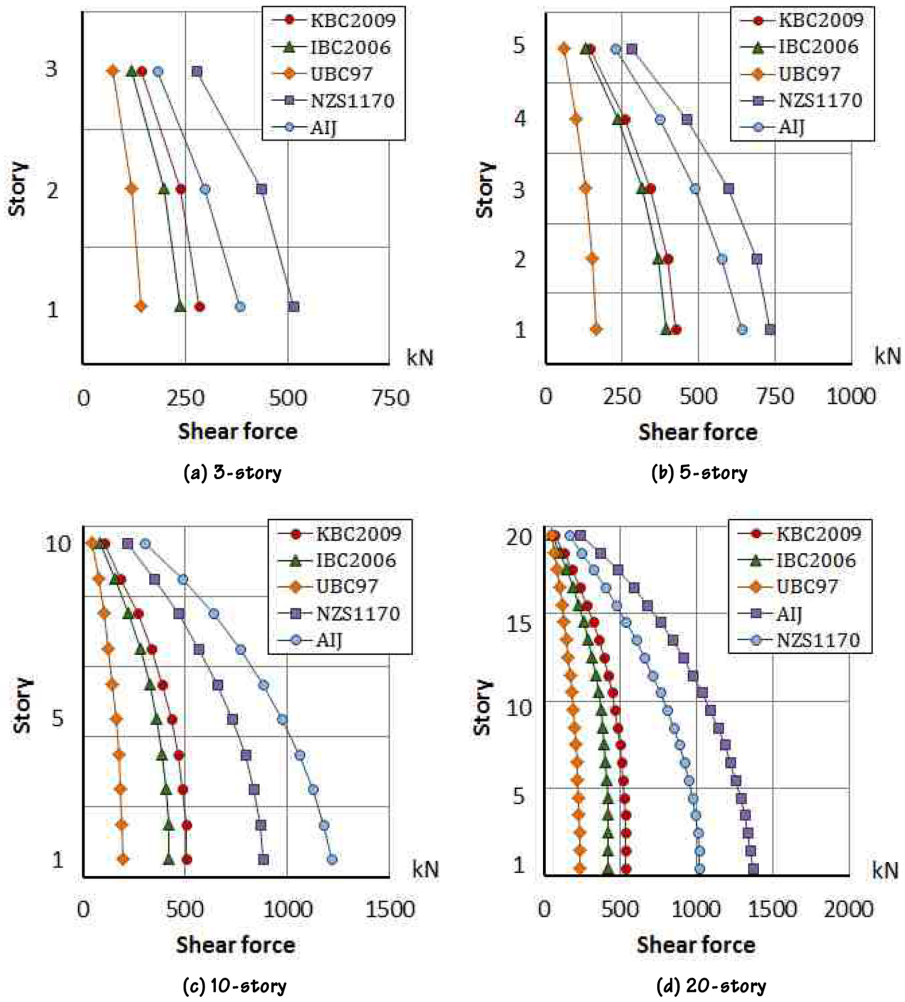


Figure 2-1. Story shear force distribution based on the seismic design code.

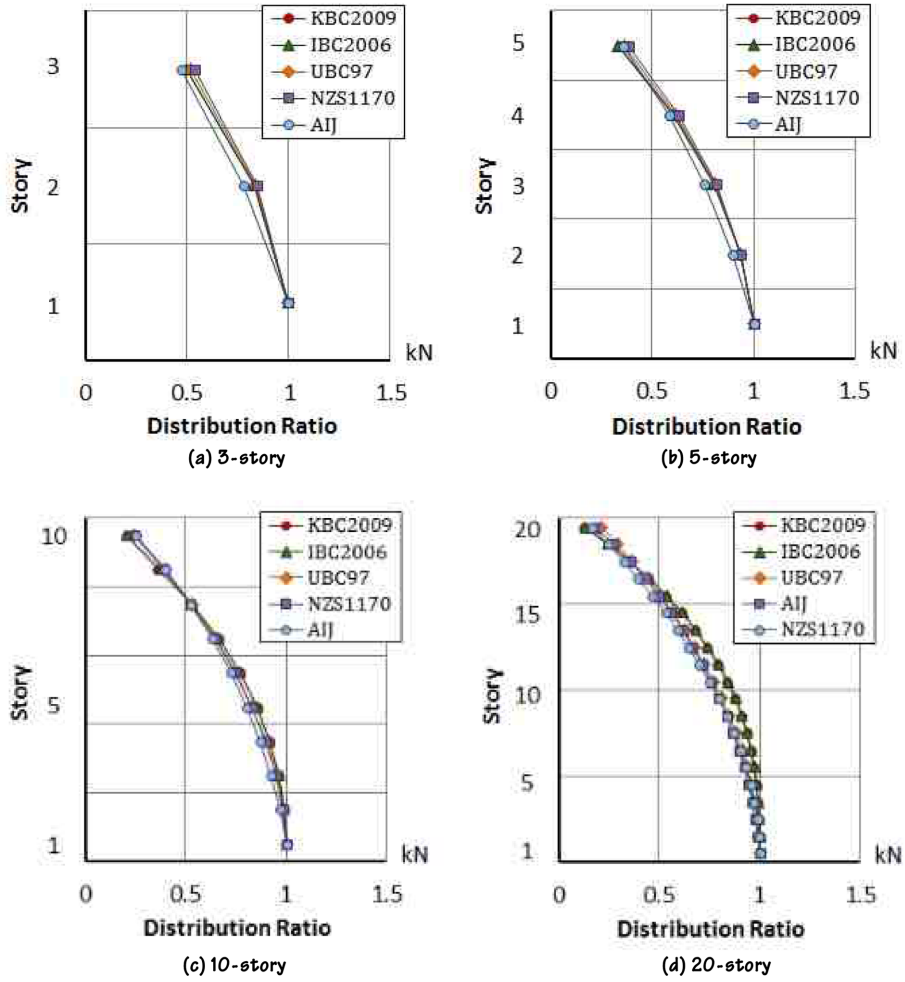


Figure 2-2. Story shear force distribution based on the seismic design code.

α_1 : Yield shear force coefficient of 1st story

Therefore, the distribution of yield shear force coefficient is non-dimensional quantity representing the strength of each structure story on valid weight to the distribution for 1st story, and can be used to compare the pattern of story shear force distributions based on seismic design code, regardless of the absolute size of base shear.

2.2.2. Cumulative plastic deformation ratio

The plastic deformation energy divided by the yield deformation energy equals to the cumulative plastic deformation ratio in dimensionless quantity value. When the load is removed, the elastic deformation disappears and the material will return to its orignal shape. On the other hand, the plastic deformation does not disappear, remains in the structure, and cumulative up to critical failure condition. In this sense, the plastic deformation energy can be used to measure the damage. The definition of cumulative plastic deformation ratio on each story η is as shown in Formula (2.7).

$$\eta_i = \frac{W_{pi}}{Q_{yi}\delta_{yi}} \tag{2.7}$$

when, W_{pi} : Plastic deformation energy on i story
Q_{yi} : Yield story shear force on i story
δ_{yi} : Yield strain on i story

2.2.3. Concept of the optimum distribution of yield story shear force coefficients

The optimum distribution of yield story shear force coefficients is to evenly distribute the damage over the structure based on the cumulative plastic deformation ratio of each story. The "Earthquake-Resistant Limit-State Design for Buildings2)" proposes the calculation formula of optimum distribution of yield story shear force coefficients, a single curve of distribution of yield story shear force coefficients on which the cumulative plastic deformation ratio appears the most constant when the vibratory ground motion of El Centro (1940) is entered, for the multi-mass system model with a resilient characteristic of perfect elasto-plasticity in which the mass distribution of each story is equalized. Fig. 2-3 shows single curves of

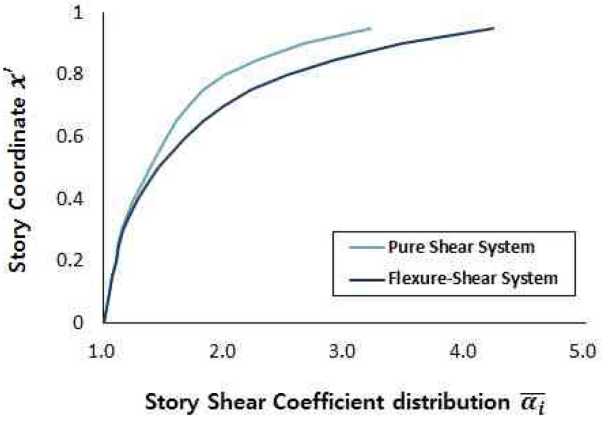


Figure 2-3. Single curve (H. Akiyama) of optimum distribution of yield story shear force coefficients.

the optimum distribution of yield story shear force coefficients for the models of the pure shear system and the flexure shear system, and the approximation formulas are as shown in the expressions, (2.8)~(2.10).

<Optimum distribution of yield story shear force coefficients at pure shear system>

(When $x'>0.2$)

$$\overline{\alpha_s}=1+1.5927x'-11.8519x'^2+42.5833x'^3 \quad (2.8)$$
$$+59.4827x'^4+3.1586x'^5$$

(When $x'<0.2$)

$$\overline{\alpha_s}=1+0.5x' \quad (2.9)$$

<Optimum distribution of story shear force coefficients at flexure shear system>

$$\overline{\alpha_b}=\overline{\alpha_s}+1.25x'^4 \quad (2.10)$$

When, $x'=\frac{x}{H}=\frac{i-1}{N}$ (2.11)

x : Height up to the story surface from the ground
H : Over-all height of structure
N : Total number of stories of structure

The distribution of yield story shear force coefficients is an indicator which refers to the ratio of the strength distribution of structure for valid weight to the 1st story, so the value of 1st story should always be 1. The story shear force of the story increases along with the value of $\overline{\alpha_i}$. The H.Akiyama's graph of optimum distribution of yield story shear force coefficients represents a curvilinear form which is incremental toward the upper portion of graph with the increased value of $\overline{\alpha_i}$, showing that the story shear force is distributed mostly on the upper portion rather than on middle or lower portions. Given the fact that this story shear force distribution is the results of considering the effects of higher vibration modes through the dynamic response analysis, the load tends to be abruptly concentrated on the upper portion of a multiple layer structure under vibratory ground motion according to the effects of higher vibration modes.

2.3. Distribution of story shear force coefficients distribution by seismic design code

The concept of distribution of yield story shear force coefficients is to show the layer strength distribution by using the yield shear force of each story. But, supposing the behavior of a structure as the perfect elasto-plasticity, the yield shear force and the story shear force can be equally applied. So, in the calculation formulas (2.5)~(2.6) of the section 2.2, we substitute the yield shear force Q_{yi} with the story shear force Q_i, propose the distribution of story shear force coefficient ${}_s\alpha_i$, and calculate the story shear force distribution of each seismic design code. The calculation formulas for the story shear force coefficient ${}_s\alpha_i$ and the distribution of story shear force coefficient ${}_s\alpha_i$ are as shown in Formulas (2.12) and (2.13) respectively.

$${}_s\alpha_i=\frac{Q_i}{\Sigma_{j=i}^{N}W_j} \quad (2.12)$$

When, Q_i : Story shear force of i story
$\Sigma_{j=i}^{N}W_j$: Total weight of the upper portion of i story

$${}_s\overline{\alpha_i}={}_s\alpha_i/{}_s\alpha_1 \quad (2.13)$$

When, ${}_s\alpha_i$: Story shear force coefficient of i story
${}_s\alpha_1$: Story shear force coefficient of i story

The Fig. 2-4 shows the distribution of story shear force coefficient according to the story shear force (Fig. 2-1) based on each seismic design code complying to the structural requirements of Table 2-4.

As to the overall shape of distribution of story shear force coefficient, the difference in the low-rise structure is not significant between the seismic design code, but the difference can be certainly identified in the high-rise structure. Comparing the patterns of shear force distribution of each seismic design criterion based on the graph of 20-story structure, they can be largely classified into linear form (KBC2009, IBC2006) and curvilinear form (UBC97, AIJ, NZS1170, H. Akiyama).

Having the distribution of linear form, both KBC2009 and IBC2006 represent the same load distribution type (refer to Table 2-2), and the distribution patterns appear almost identically. On the other hand, showing in curvilinear form, the distributions of UBC97, NZS1170, AIJ and H. Akiyama's have the different types of calculation formulas, and show the different patterns of distribution. As to the distributions of UBC97 and H. Akiyama's, an inc-

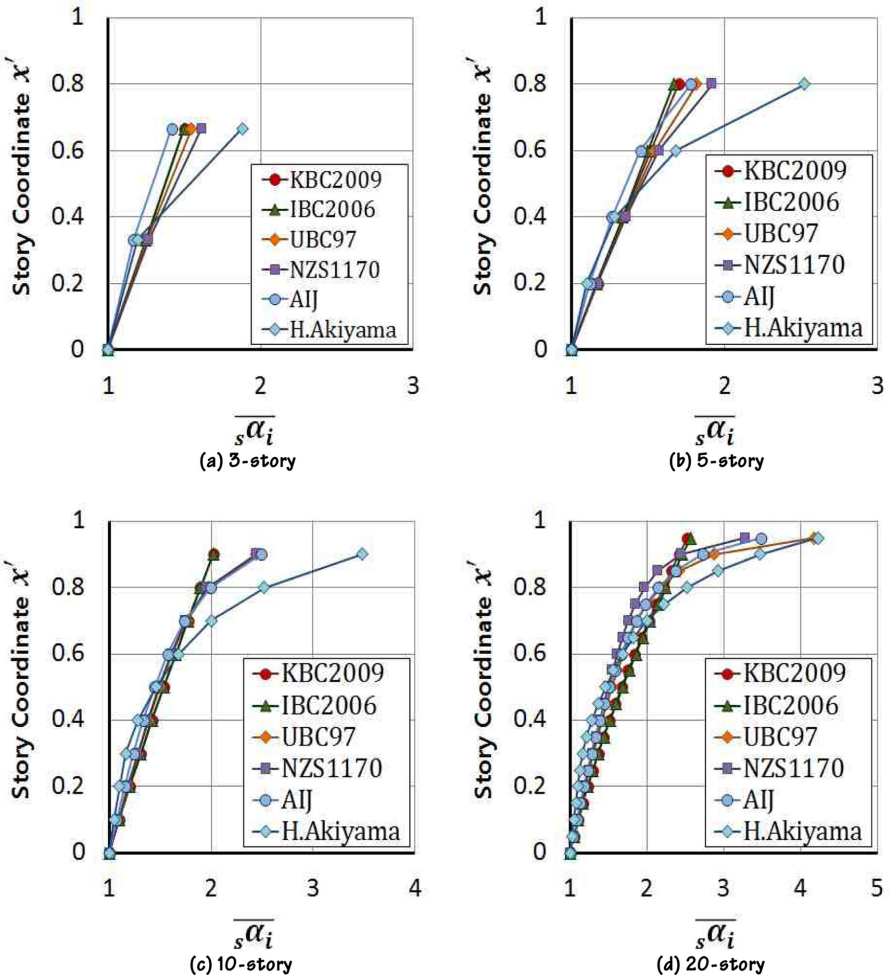


Figure 2-4. Distribution of story shear force coefficient of each seismic design code.

rease of shear force is higher in top portion, and the shear force distribution of NZS1170 is lower in upper-middle. Although the load bearing distribution of H. Akiyama's is the lowest in lower portion, the shear force starts to increase from middle portion and shows the highest shear force distribution in top portion, showing the most fluent curve compared to other criteria.

3. Response Analysis of Structure according to Story Shear Force Distribution

3.1. Analytical model design

Considering the nature of distribution of story shear force coefficient, which appears in the story-specific distribution, a beam with infinite stiffness and the 2D framework were applied to the model shape for response analysis in order to facilitate the story-specific design and the analysis of response characteristics. Thus, the response of columns represents the corresponding story, and the story shear force distribution based on a seismic design criterion can be reflected to designing the analytical model by controlling the load bearing of columns. The basic shape of the analytical model is as shown in Fig. 3-1.

Provided the damage is concentrated in the hinge area of both ends of column member, the framework was modelled with flexure spring on both ends of column member as shown in Fig. 3-2. The resilient characteristic of flexure spring was set to bi-linear of perfect elasto-plasticity as shown in Fig. 3-3.

As mentioned earlier in the paper, the Formulas from (2.12) to (2.13) were proposed for calculating the distribution of story shear force coefficient. And, they can be

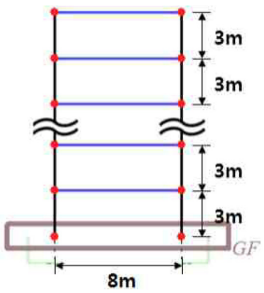


Figure 3-1. Analytical model.

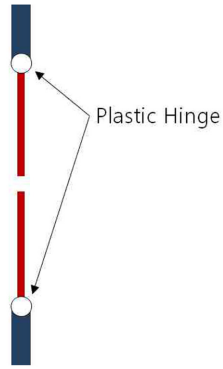


Figure 3-2. Modeling of column member.

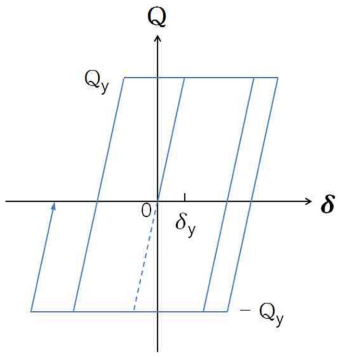


Figure 3-3. Resilient characteristic of perfect elasto-plasticity.

summarized for the story shear force Q_i as shown in Formula (3.1).

$$Q_i = {}_z\alpha_1 \, {}_s\overline{\alpha_i} \, \Sigma_{j=i}^{N} W_j \tag{3.1}$$

When, ${}_z\alpha_1$: Story shear force coefficient on 1st story according to the local conditions

${}_s\overline{\alpha_i}$: Distribution of story shear force coefficient on i story

$\Sigma_{j=i}^{N} W_j$: Total weight of upper structure on i story

The factor ${}_z\alpha_1$ defines the size of the base shear of a structure. Since the ground conditions and the scale of the expected earthquake are different depending on the region, the value of ${}_z\alpha_1$ should be applied accordingly. This

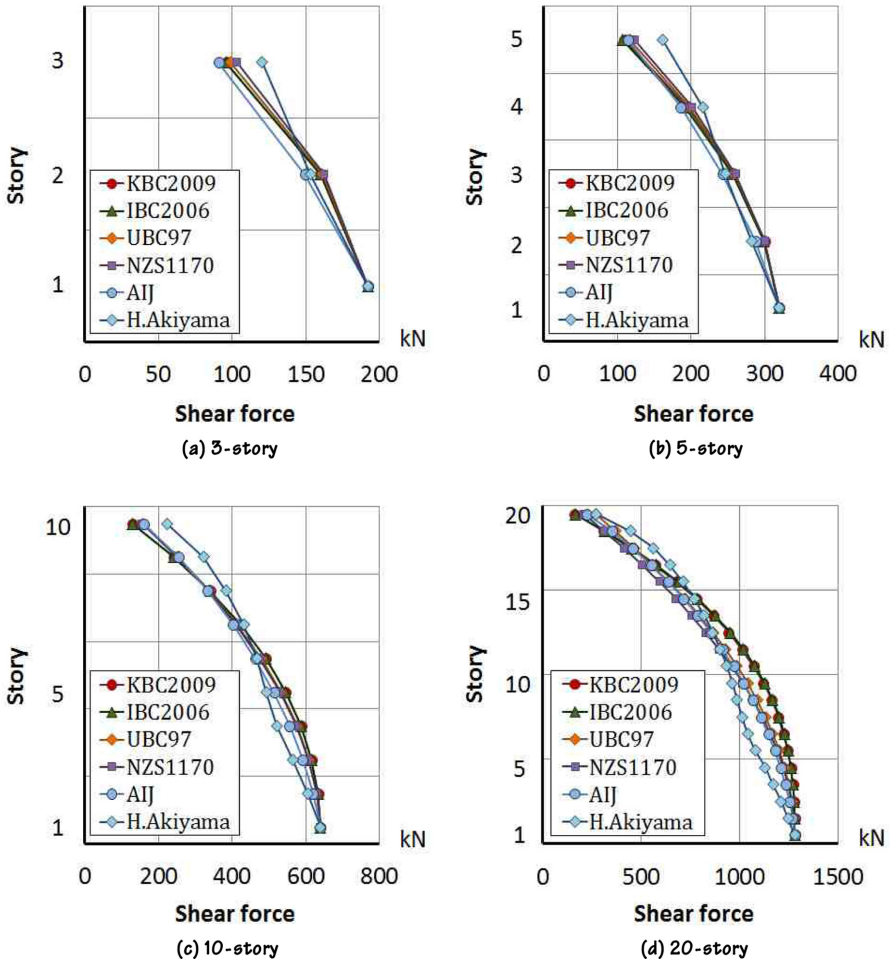


Figure 3-4. Redesigned story shear force based on distribution of story shear force coefficient.

study is based on the domestic regional conditions, and the number 0.1 was applied to all analytical models considering that the ${}_z\alpha_1$ values of buildings (three-story to twenty-story) vary between 0.07 and 0.14.

After applying the distribution of story shear force coefficient based on each seismic design criterion to the proposed formula, as shown in Formula (3.1), the result of remodeling the story shear force distribution of each analytical model is as shown in Fig. 3-4.

As to the distribution of the story shear force of each analytical model, the story shear force of the models KBC 2009 and IBC2006 with low load bearding increase appears high in middle as well as lower portions and low in upper portion compared to other criteria. The shear force distributions of the models UBC97, NZS1170, AIJ and H. Akiyama drastically increase in upper portion, and tend to be concentrated in top portion. The H. Akiyama's model has a noticeable difference in which the story shear force is low in lower portion and high in upper portion appearing in tertiary curve.

The size of the framework member was designed by using the story shear force of the each analytical model calculated based on the distribution of story shear force coefficient. As shown in Fig. 3-5, the load on each story is concentrated on both columns, so the story shear force Q_i is the entire external force acting upon the column members.

The resilient characteristic of column was set based solely upon the premise of bending deflection, so the full plastic moment was calculated based on the plastic design method. The process of calculating the full plastic moment is as shown in Formulas (3.2) to (3.3), subject to the condition that the number of plastic hinge occurring on both columns is 4.

$$Q_i \cdot h_i = 4M_p \tag{3.2}$$

$$M_p = \frac{Q_i}{4} \cdot h_i \tag{3.3}$$

When, Q_i : Story shear force of i story
h_i : Story height of i story

We found the plastic section modulus of column from the full plastic moment M_p of the calculated column and designed the section size of corresponding framework member. The section size of the designed framework member is included in Appendix 2. The framework member is square-shape steel pipe, and the used material is SS400 (F_y = 235 N/mm^2).

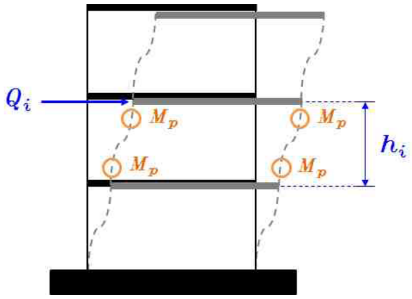


Figure 3-5. Load action diagram for designing the framework member columns.

3.2. Analysis method

3.2.1. Static elasto-plastic analysis

The static elasto-plastic analysis was carried out in the manner of calculating the seismic load of each story according to the conditions of analytical model as well as loading at the bottom of each story as shown in Fig. 3-6.

Table 3-1 shows the story deformation angle at limit state presented by the domestic and international design code. We defined that the limit state was reached when the maximum story deformation angle of analytical model reached at 1/50 of the story deformation angle safety limit when the following factors hold true: first, the minimum limit state of a structure becoming prefectly plastificated is the safety limit. Second, the story deformation angle safety limit ranges between 1/30 and 1/75.

*The nonlinear response analysis program, CANNY (Ver. C11), which is capable of both static and dynamic analyses, the energy input of the entire structure as well as measuring the plastic deformation energy for framework member.

3.2.2. Dynamic response analysis

The analysis program CANNY is based on the Newmark-β method for the dynamic response analysis. Applying β=0.25 and γ=0.5 in this study, we received the same results as in the linear acceleration method. The damping ratio of frame is considered as 2%.

The "Seismic design of a structure according to Energy Balance Method" defines the state of perfect plasticity as η=10 level, where η is the cumulative plastic deformation ratio of the plastic deformation capacity of structural member. Conservatively applying η=6 as the limit state in this study, we conducted the analysis by multiplying the acceleration ratio to the input earthquake motion until the value of the cumulative plastic deformation ratio on each story reached 6 at the maximum.

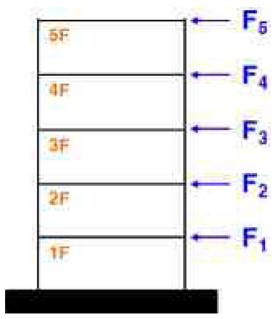


Figure 3-6. Static elasto-plastic analysis overview.

Table 3-1. Story deformation angle at limit state

Performance limit (frame)	USA		Japan		South Korea
	SEAOC Vision2000	SAC - FEMA	Damage & Disaster Criteria	Japan Society of Professional Engineers	KBC2009
Functional limit	-	-	-	1/200	-
Damage limit	-	-	1/150	1/150	1/100
Recovery limit	1/200	1/100	1/100	1/100	-
Safety limit	1/40	-	1/30	1/75	1/67
Collapse	-	-	-	-	1/50

Table 3-2. Characteristics of prominent period of input earthquake motion

Seismic wave	Peak ground acceleration (gal)	Prominent period elements (Sec)
El Centro NS (1940)	341	0.463, 0.681, 0.867
Hachinohe NS (1968)	225	0.947, 1.125, 2.770
Kobe NS (1995)	834	0.350, 0.688, 0.838
Taft EW (1952)	176	0.336, 0.422, 0.439

For the comprehensive analysis on the response information of a structure for a variety of period elements, we used the input earthquake motions of El Centro NS, Hachinohe NS, Kobe NS and Taft EW, which are widely used in seismic design and study.

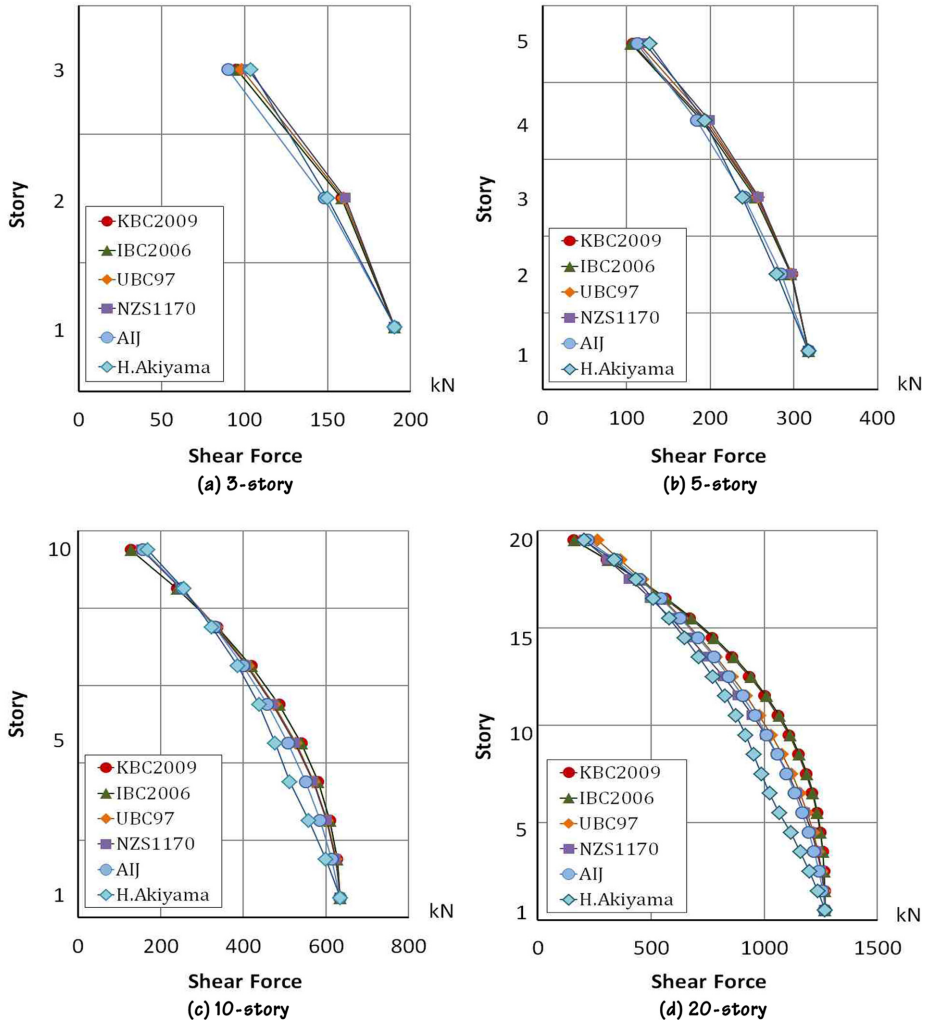


Figure 3-8. Response shear force distribution by static elasto-plastic analysis.

3.3. Analysis result

3.3.1. Static elasto-plastic analysis

The response shear force graph of each seismic design code based on the static elasto-plastic analysis is as shown in Fig. 3-8. The response shear forces are not that different depending on the seismic design code, but they are somewhat different in high-rise models. Based on the 20-story analytical model, the response shear forces of KBC 2009 and IBC2006 appear high in middle portion, and those of UBC97, NZS1170, AIJ and H. Akiyama appear low in middle portion with high in upper portion. As to the response shear force in top portion, UBC97 was the most prominent. The H.Akiyama's distribution was a little lower than those of other criteria, but its response shear force in upper portion was at a level comparable with others.

The distribution trend of response shear force by static elasto-plastic analysis appeared almost similar to the analysis results of story shear force graph (refer to Fig. 3-4). This was because the effects of higher vibration modes were not properly reflected according to the seismic load due to the stress redistribution occurring under the static load. Thus, the response characteristics analysis by static elasto-plastic analysis was just to confirm the load-carrying

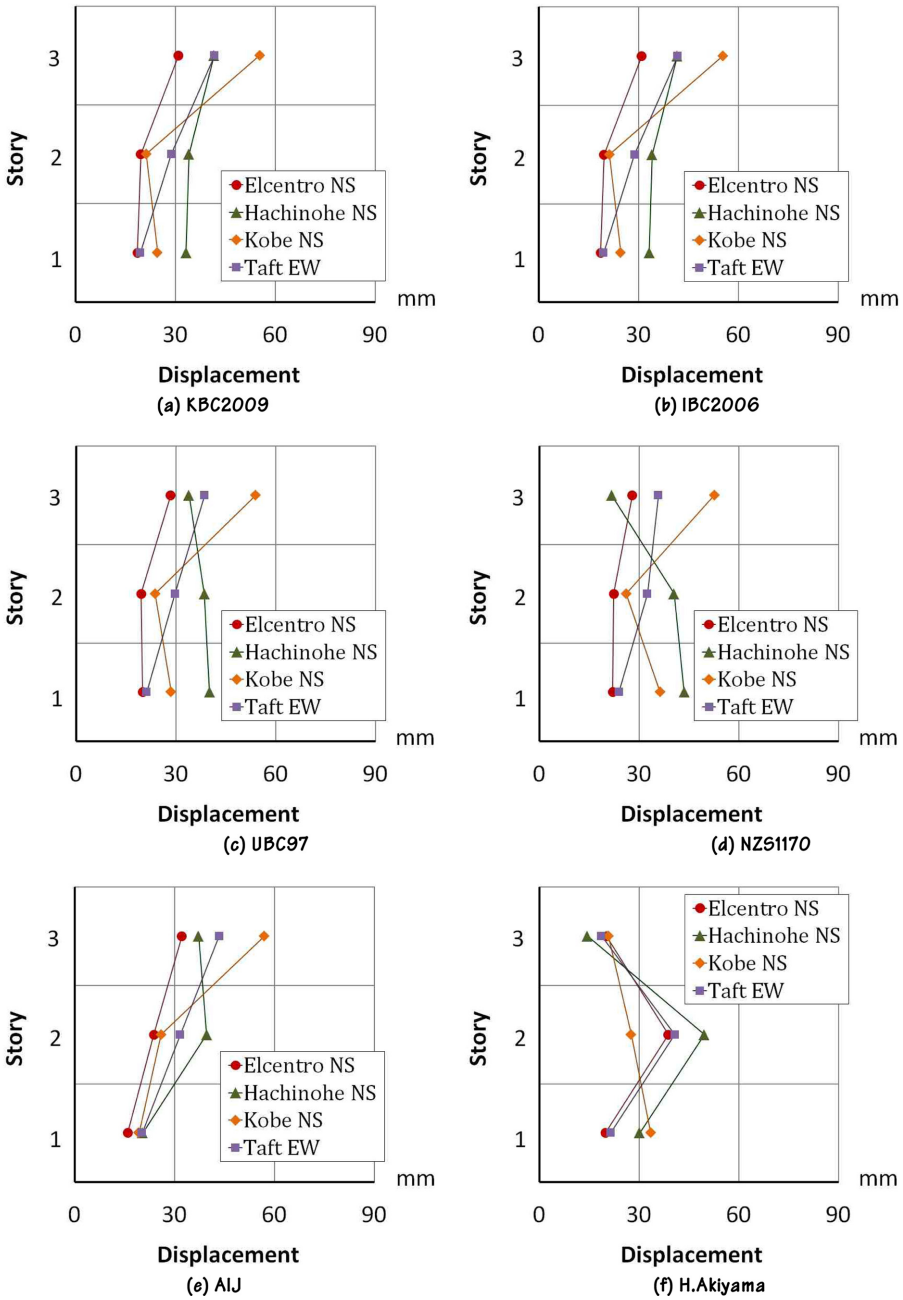


Figure 3-13. Maximum relative story displacement distribution by dynamic response analysis (3-story).

capacity of each story and thought to have low reliability as an indicator in verifying the seismic performance of a structure.

3.3.2. Dynamic response analysis

The maximum relative story displacement of a story-specific analytical model by dynamic response analysis is as shown in Figs. 3-13 to 3-14. In case of 3-story model, the models KBC2009 and IBC2006 show the relatively uniform distribution of relative story displacement, and the H. Akiyama model, which distributed the shear force the most in upper portion, shows its displacement tended to be somewhat less concentrated in middle portion. But, as the number of stories increased, the distribution of relative story displacement of analytical model, which increased the load bearing in upper portion, tended to appear in even distribution. As to the KBC2009 and IBC 2006 models, the displacements were concentrated in upper portions, and the H. Akiyama model showed the displacement was dispersed toward the upper portion moving from the concentrated middle-lower portions.

The deformation occurring section of the maximum relative story displacement graph for the 20-story model was consistent with most of the expected stress concentra-

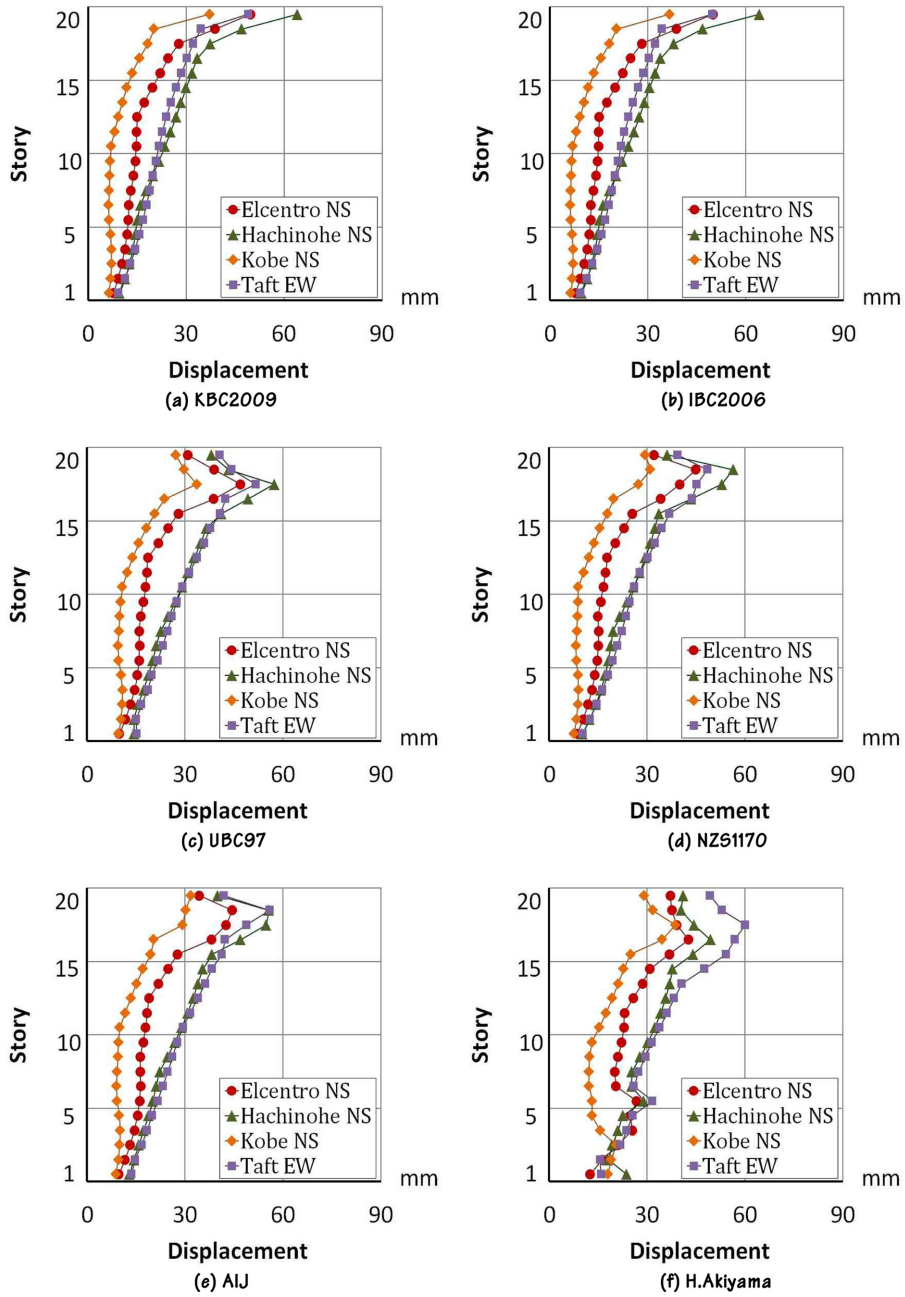


Figure 3-14. Maximum relative story displacement distribution by dynamic response analysis (20-story).

tion section. In case of KBC2009 and IBC2006 models, in which the greater part of stress was concentrated in top portions, the plastic deformation occurred rapidly in top portions. Although the plastic deformation also occurred in upper portions of UBC97, NZS1170 and AIJ models, the sections of plastic deformation appeared in wider areas because those models had larger sections of stress concentration, compared to KBC2009 and IBC2006. The plastic deformation also occurred in bottom portion of UBC 97 model. In case of H. Akiyama model, the plastic deformation occurred in upper and lower portions in a relatively wide range. Therefore, we can identity that the plastic deformation evenly occurs as the effects of higher vibration modes increase because the stress of analytical model, which increased the load bearing in upper portion, is dispersed.

The analysis results of the response shear force and relative story displacement by dynamic response analysis clearly showed the impact of the dynamic loading, and the response characteristics according to the story load bearing distribution of each seismic design criterion were clearly distinguished. Accordingly, by measuring the cumulative plastic deformation energy of a structure after these characteristics, we analyzed the characteristics of

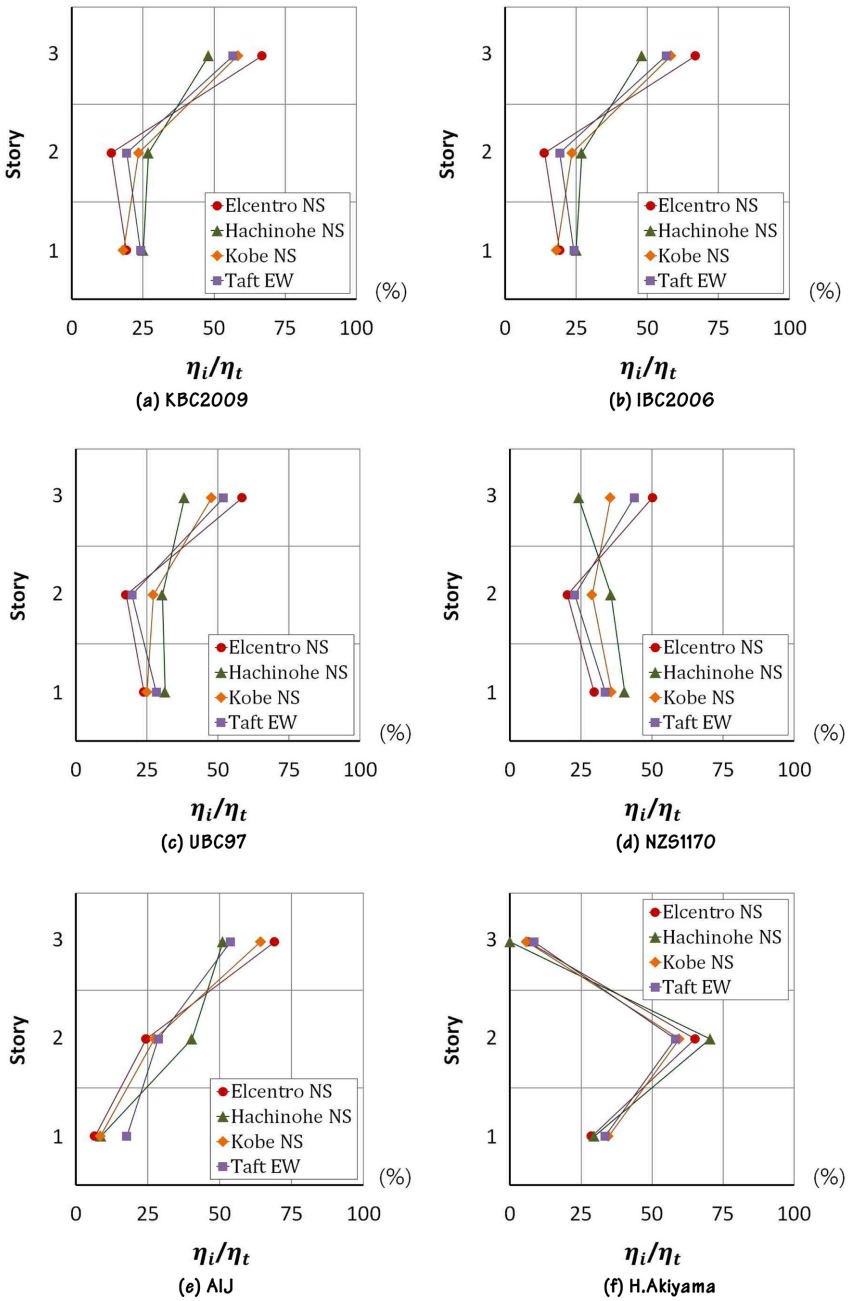


Figure 3-15. Distribution of cumulative plastic deformation ratio (3-story).

layer damage distribution based on each seismic design criterion. As for the damage assessment criterion, the cumulative plastic deformation ratio (refer to Formula 2.7) by plastic deformation energy at limit state was used, and the story distribution values for the cumulative plastic deformation ratio of the entire structure are as shown in Figs. 3-15 to 3-18.

The overall layer damage distribution showed similarities to the graph of maximum relative story displacement, but showed the damage concentration due to the cumulative plastic deformation. In case of 3-story model, some damage was concentrated on upper portions of KBC2009 and IBC2006 models, while AIJ model showed the distribution on 1st story the least, and most damage was concentrated on 2nd story of H.Akiyama model unlike other criteria.

The patterns of the damage distribution based on the seismic design code were clearly identified from 5-story analytical model and above. In KBC2009 and IBC2006 models, most damage was concentrated in top portions, but the damage concentration was somewhat mitigated in UBC97, NZS1170, AIJ and H. Akiyama models. In UBC 97, NZS1170 and AIJ models, damage was concentrated in upper and bottom portions in some degree, but the con-

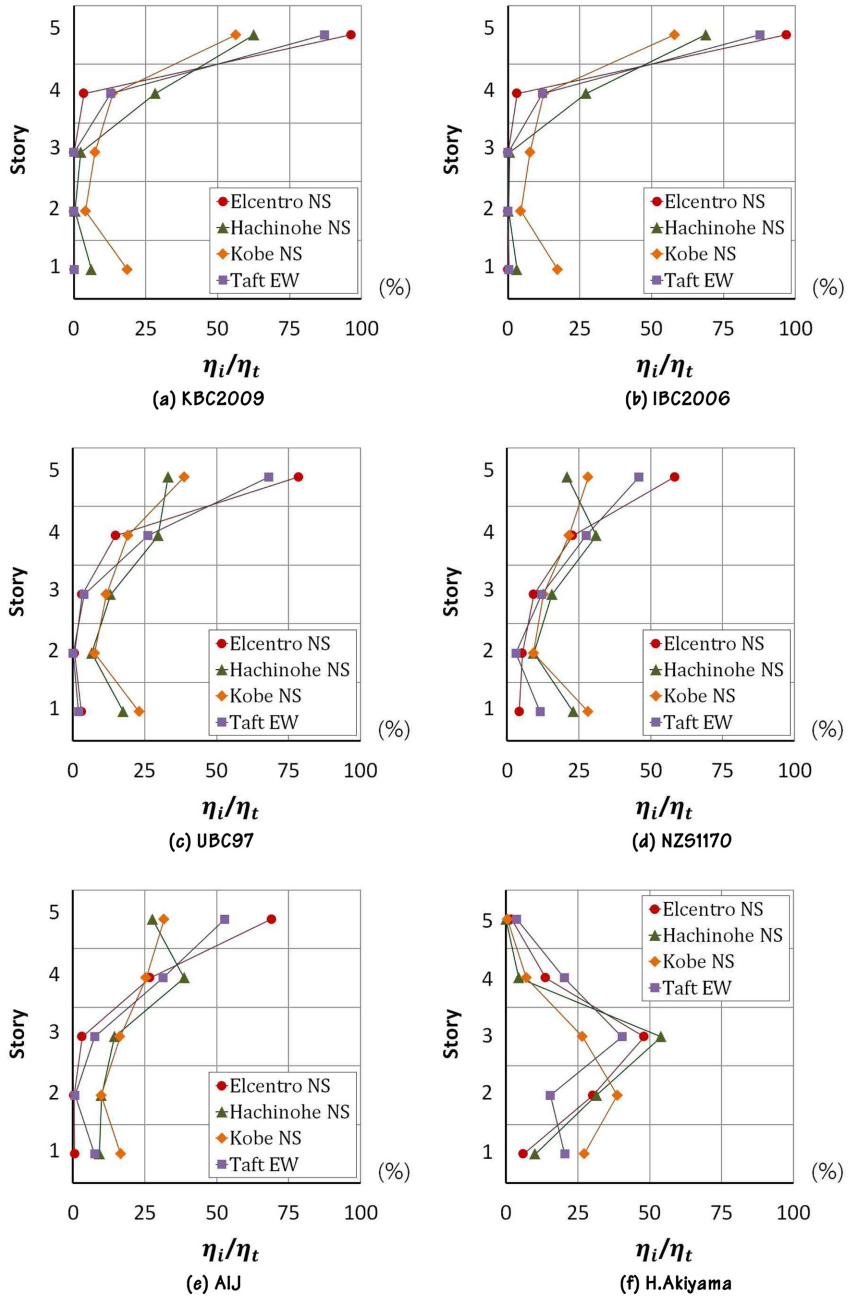


Figure 3-16. Distribution of cumulative plastic deformation ratio (5-story).

centration level was lower than those of KBC2009 and IBC2006 models. In H. Akiyama model, the damage distribution appears significantly in middle portions of both 5-story and 10-story structures unlike other criteria. However, the 20-story structure showed the most stable damage distribution: the load carrying almost disappeared in middle portion, the damage was distributed in upper and lower portions, and concentrated more in lower portion unlike other criteria.

As it was studied during the analysis process of distribution of story shear force coefficient, the layer damage distribution of each analytical model clearly showed the differences in reflecting the degree of load bearing increase in upper portion. The KBC2009 and IBC2006 models with less distribution of load bearing in upper portions showed high stability in low-rise models, and the damage was extremely concentrated in top portions as the number of stories increases. The more the load bearing distribution had in upper portion of a model, the more evenly the damage distribution appeared in middle and high-rise models. In particular, H. Akiyama model with the highest load bearing in upper portion showed some damage concentration in lower portion and the most stable damage distribution on 20th story.

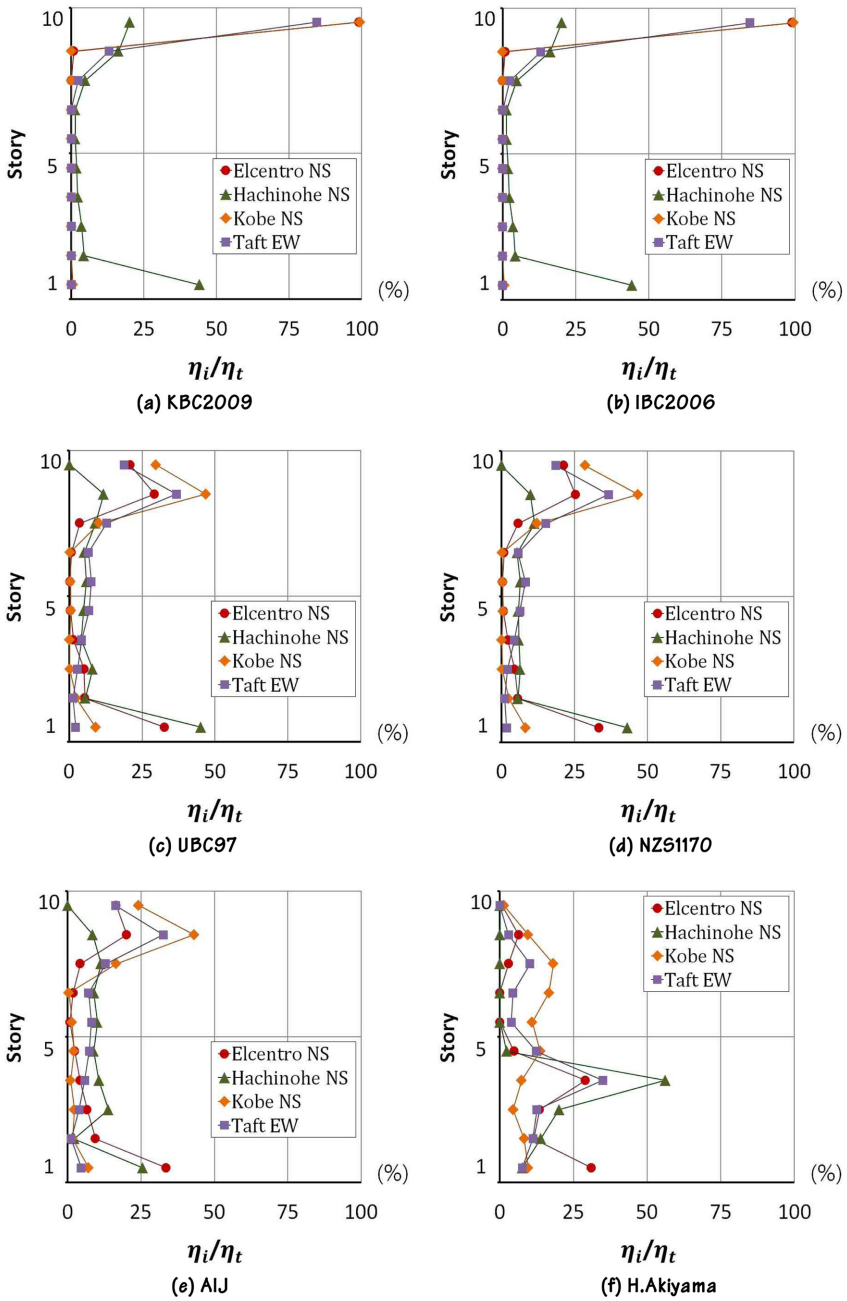


Figure 3-17. Distribution of cumulative plastic deformation ratio (10-story).

The analysis on characteristics of damage distribution can be used to accurately analyze the damage concentration tendency of each analytical model, but is not suitable for showing the seismic efficiency of analytical model itself. Therefore, we analyzed the seismic efficiency by measuring the energy absorption of each analytical model at limit state. The energy absorption of each analytical model at limit state is as shown in Fig. 3-19.

The higher the numerical value of the axis of ordinates, the higher the seismic efficiency will be. In lower models, the difference in energy absorption by analytical model rarely appeared, and most values were distributed in 25~50 kN·m range. But, as the number of stories increased, the seismic efficiency of the models KBC2009 and IBC 2006 relatively decreased, and that of the models UBC97, NZS1170, AIJ and H. Akiyama increased. Especially, the increase was noticeable in H. Akiyama model, and 20-story model turned out to be capable of absorbing at least two times or more energy compared to the KBC2009 model. The analysis results of energy absorption at limit state showed that a model with the enhanced shear force in upper portion tend to have higher seismic efficiency, and was not affected much by a load bearing distribution type.

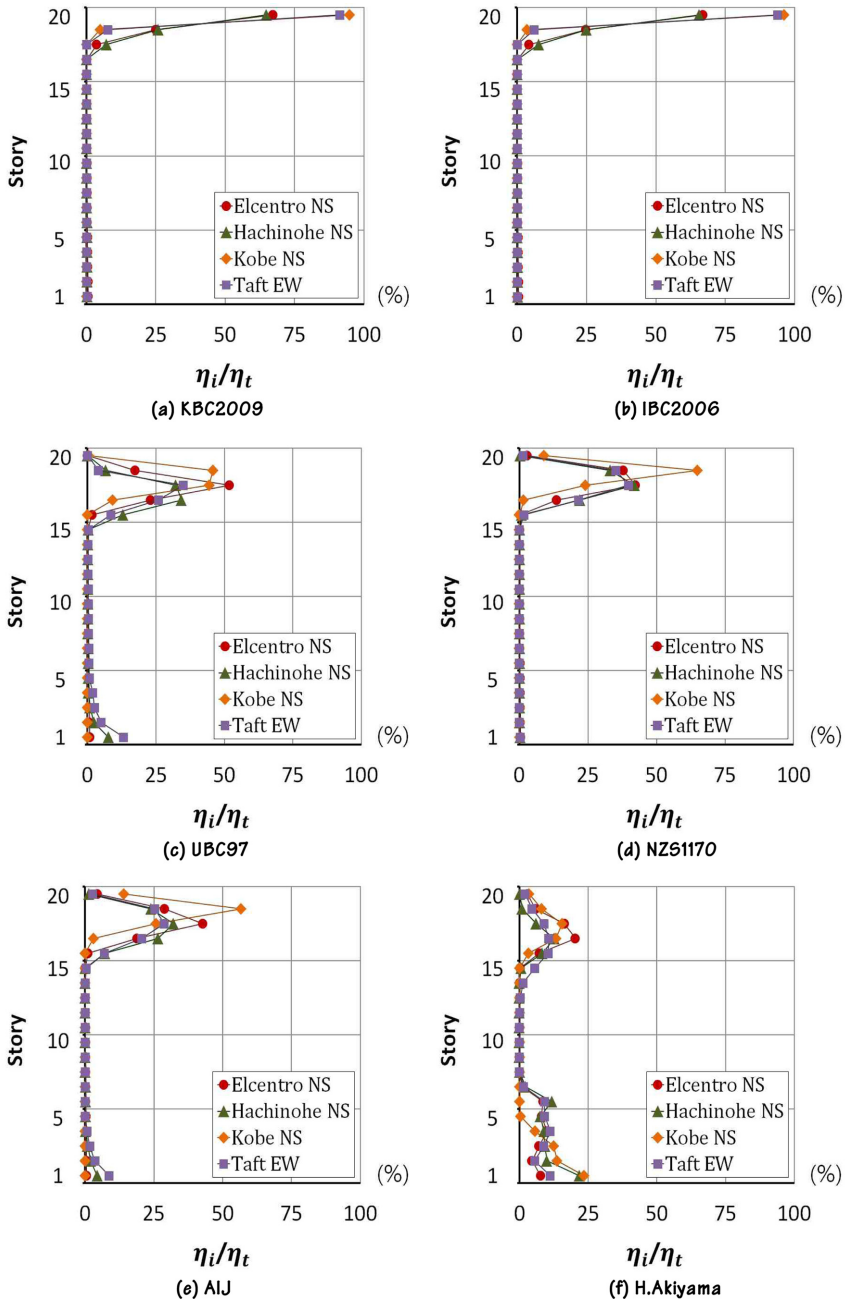


Figure 3-18. Distribution of cumulative plastic deformation ratio (20-story).

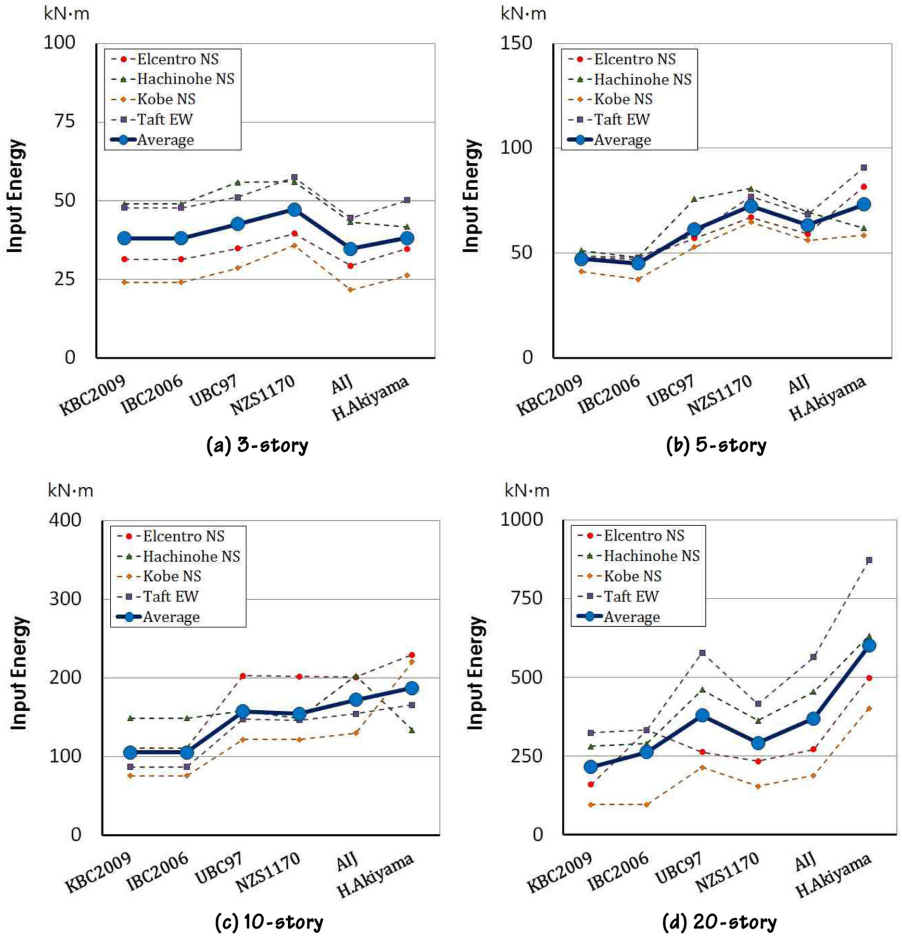


Figure 3-19. Energy absorption at limit state.

4. Optimum Distribution of Story Shear Force Coefficients

On the response characteristics analysis of a structure in accordance with the story shear force distribution of domestic and international seismic design code, we found that the seismic safety of a structure was largely affected by the shear force distribution in upper portion of higher-rise model, through this, we were able to predict the distribution tendency of story shear force affected by higher vibration modes to a certain extent.

Based on the design and the layer damage analysis methods of analytical model proposed in this study, we draw the optimum distribution of story shear force coefficient which shows a steady layer damage distribution for various analytical models, and propose a calculation formula for the optimum distribution of story shear force coefficient by analyzing the tendency. In addition, by applying the proposed calculation formula, we analyze the characteristics of layer damage distribution of the designed structure, compare with the existing seismic design code, and verify the validity of the proposed calculation formula.

4.1. Induction of optimum distribution of layer damage

As to the distribution pattern of graph, the higher-rise model is more likely to show low in the shear force distribution of middle portion, and fluctuating sharply in accordance with the input earthquake motion. As for the optimum distribution of story shear force coefficient, the high level seismic safety with respect to various input earthquake motions should be granted, so the need to draw a generalized curve, including the optimum distribution of story shear force coefficient in accordance with each input earthquake motion, arises.

4.2. Calculating the optimum distribution of story shear force coefficients

4.2.1. How to estimate the optimum distribution of story shear force coefficients

The calculation formula for story shear force (3.1) using the distribution of story shear force coefficient and the weight of upper structure. By counter-plotting the calculation process of story shear force, summarizing the Formula (3.1) for the coefficient distribution $_s\overline{\alpha}_i$, and applying the story shear force $_pQ_i$ in the state of optimum distribution of layer damage will yield the optimum distri-

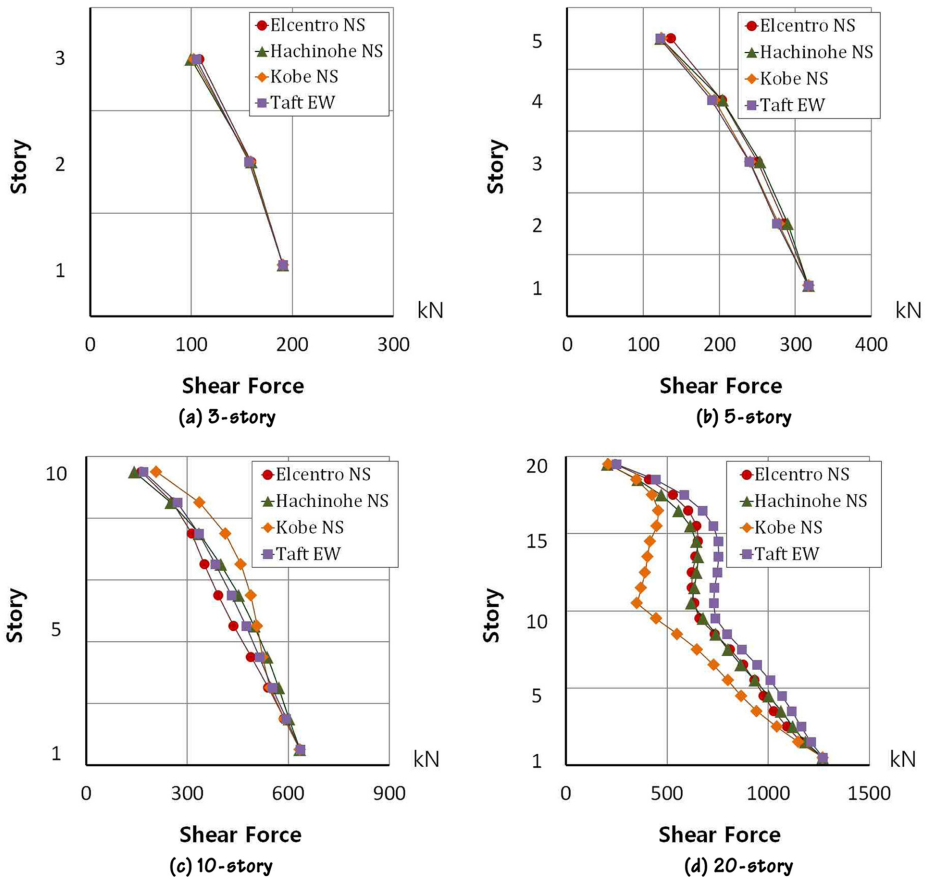


Figure 4-1. Story shear force distribution in the state of optimum distribution of layer damage.

bution of story shear force coefficient, ${}_p\overline{\alpha_i}$. The calculation formula of optimum distribution of story shear force coefficient is as shown in Formula (4.1).

$$ {}_p\overline{\alpha_i} = \frac{{}_pQ_i}{{}_z\alpha_1 \Sigma_{j=i}^{N} W_j} \tag{4.1} $$

When, ${}_p\overline{\alpha_i}$: Optimum distribution of story shear force coefficient

${}_pQ_i$: Story shear force of i story in the state of optimum distribution of layer damage

${}_z\alpha_1$: Story shear force coefficient of 1st story depending on local conditions

$\Sigma_{j=i}^{N} W_j$: Total weight of upper portion of i story

By using the above formula, the optimum distribution of story shear force coefficient ${}_p\overline{\alpha_i}$ in accordance with each input earthquake motion is estimated, and the graph is as shown in Fig. 4-2.

A look at the tendency according to the number of stories of analytical model suggests that the optimum distribution of story shear force coefficient in 3-story model is in almost linear fashion, and the higher-rise model is more likely to show a decrease in story shear force from lower portion to middle portion and a big increase in the shear force distribution. In the extreme case of 20-story model, the distribution of story shear force coefficient was estimated less than 1 in middle portion. In addition, the distribution pattern according to each input earthquake motion appeared in many forms, but the corresponding tendency was not clearly identified.

4.2.2. Drawing generalized curves

In order to comprehensively reflect the characteristics of optimum distribution of story shear force coefficient graph for each input earthquake motion, we drew the approximation formula of quadric function representing the correlation between the layer coordinates and by using the least square method. In the process, we applied 1 to all the sections where the distribution of story shear force coefficient was less than 1. The generalized curve of optimum distribution of story shear force coefficient calculated is as shown in Fig. 4-3. As to the generalized curve of optimum distribution of story shear force coefficient, the higher-rise analytical model is more likely to show an increase in distribution value of top portion and the curvature of the curve.

4.3. Proposal and verification of optimum distribution of story shear force coefficient

In the drawing result of generalized curve graph for op-

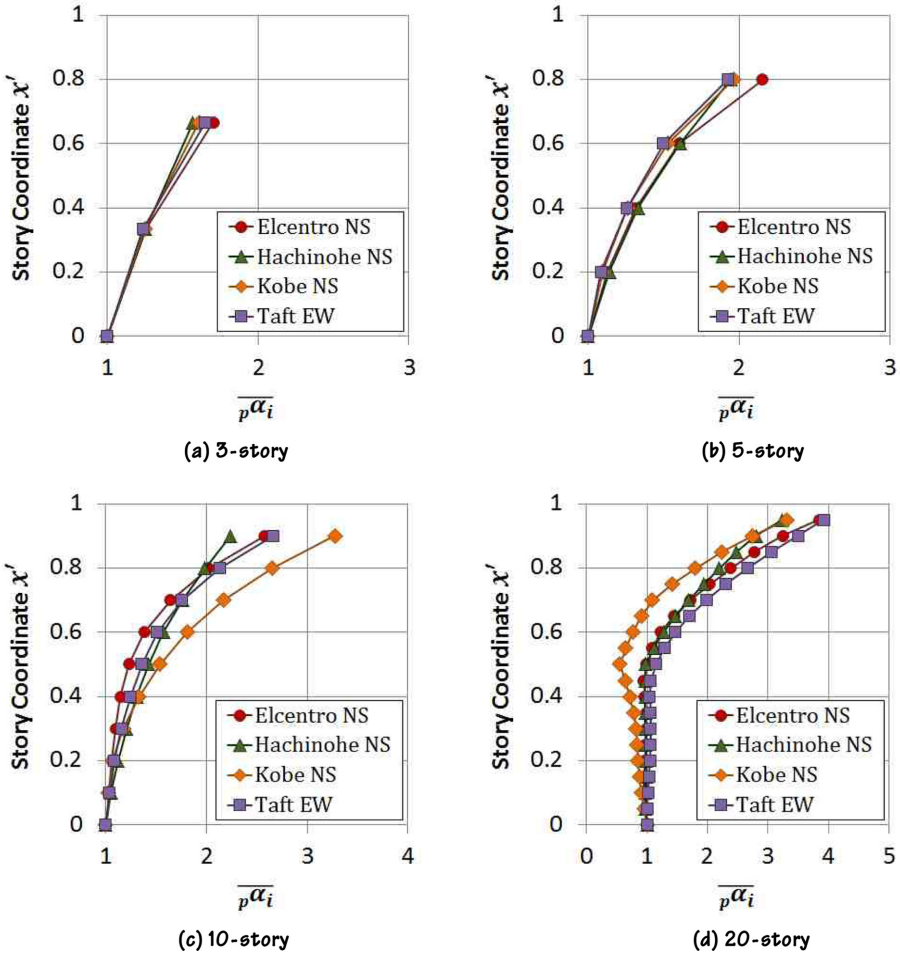


Figure 4-2. Optimum distribution of story shear force coefficient.

timum distribution of story shear force coefficient, the distribution value and the curvature of the curve according to the analytical model's story clearly showed a pattern. In general, the number of stories in a structure is proportional to the natural vibration period, so the calculation formula can be proposed by analyzing the pattern of optimum distribution of story shear force coefficient according to a variety of natural vibration periods.

4.3.1. Pattern analysis and proposal of calculation formula

Before analyzing the pattern of generalized curve according to the natural vibration period of analytical model, we measured the natural vibration period of the model designed by applying the generalized curve of optimum distribution of story shear force coefficient, and displayed as shown in Table 4-1.

It turned out that the natural vibration period of analytical model for this study appeared to have relatively large value compared to that of a general structure. Thus, we added analytical models with realistic natural vibration periods for the aspect ratios of structures, and analyzed the tendency of optimum distribution of yield story shear force coefficients accordingly. The natural vibration periods of added models are as shown in Table 4-2.

Accordingly, we found the generalized curve for optimum distribution of story shear force coefficient by using the least square method for the final 8 models as shown in Fig. 4-4.

The generalized curve of optimum distribution of story shear force coefficient drawn in accordance with a variety of natural vibration periods showed the longer the natural vibration period is more likely to clearly show an increasing pattern of the distribution value and the curvature of graph in top portion. As shown in Fig. 4-5, we showed the optimum distribution of story shear force coefficient and the natural vibration period in overlapped manner and analyzed the pattern accordingly.

The generalized curve of optimum distribution of story shear force coefficient follows the shape of an exponential function graph having the minimum value of 1. Setting an approximation formula, “” with variables A (maximum value of) and B (=curvature of curve), we drew the variable values in the most similar form to the optimum distribution of story shear force coefficient of each analytical model. As a result, we found that the variables of the

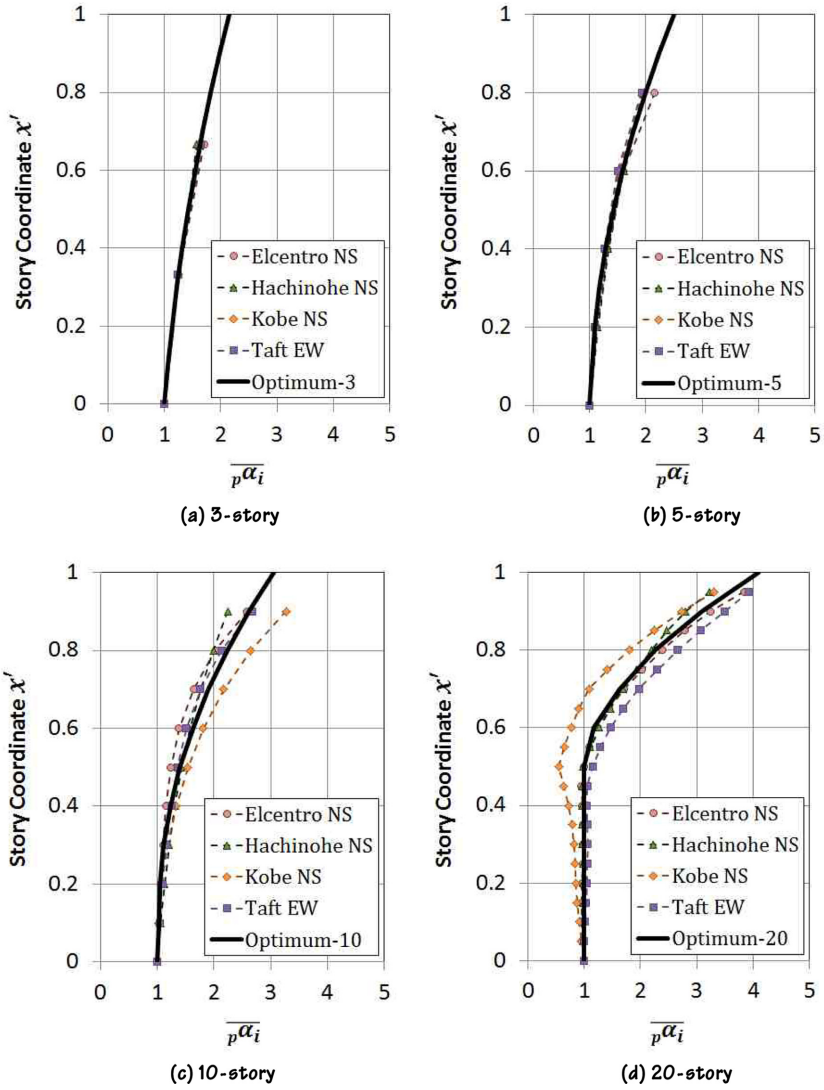


Figure 4-3. Generalized curve of optimum distribution of story shear force coefficient.

Table 4-1. Natural vibration period of model by optimum distribution of story shear force coefficient

Optimum	3-story	5-story	10-story	20-story
Natural vibration period	1.10s	1.30s	1.89s	3.87s

Table 4-2. Natural vibration period of added models

Optimum	3-story	5-story	10-story	20-story
Natural vibration period	0.40s	0.61s	1.00s	2.08s

approximation formula were in the most similar form to the optimum distribution of story shear force coefficient when they were equal to the values as shown in Table 4-3.

In addition, the variable values for the natural vibration period of analytical models are as shown in Fig. 4-6, and the patterns of variables are described in approximation formulas of quadric functions using the least square method. The approximation formulas of variables according to the analysis results are as shown in Formulas (4.2) and (4.3).

$$A = -0.08 \times T^2 + 1.05 \times T + 0.60 \tag{4.2}$$

$$B = 0.03 \times T^2 + 0.80 \times T + 0.87 \tag{4.3}$$

When, T : Natural vibration period

Thus, the calculation formula of optimum distribution

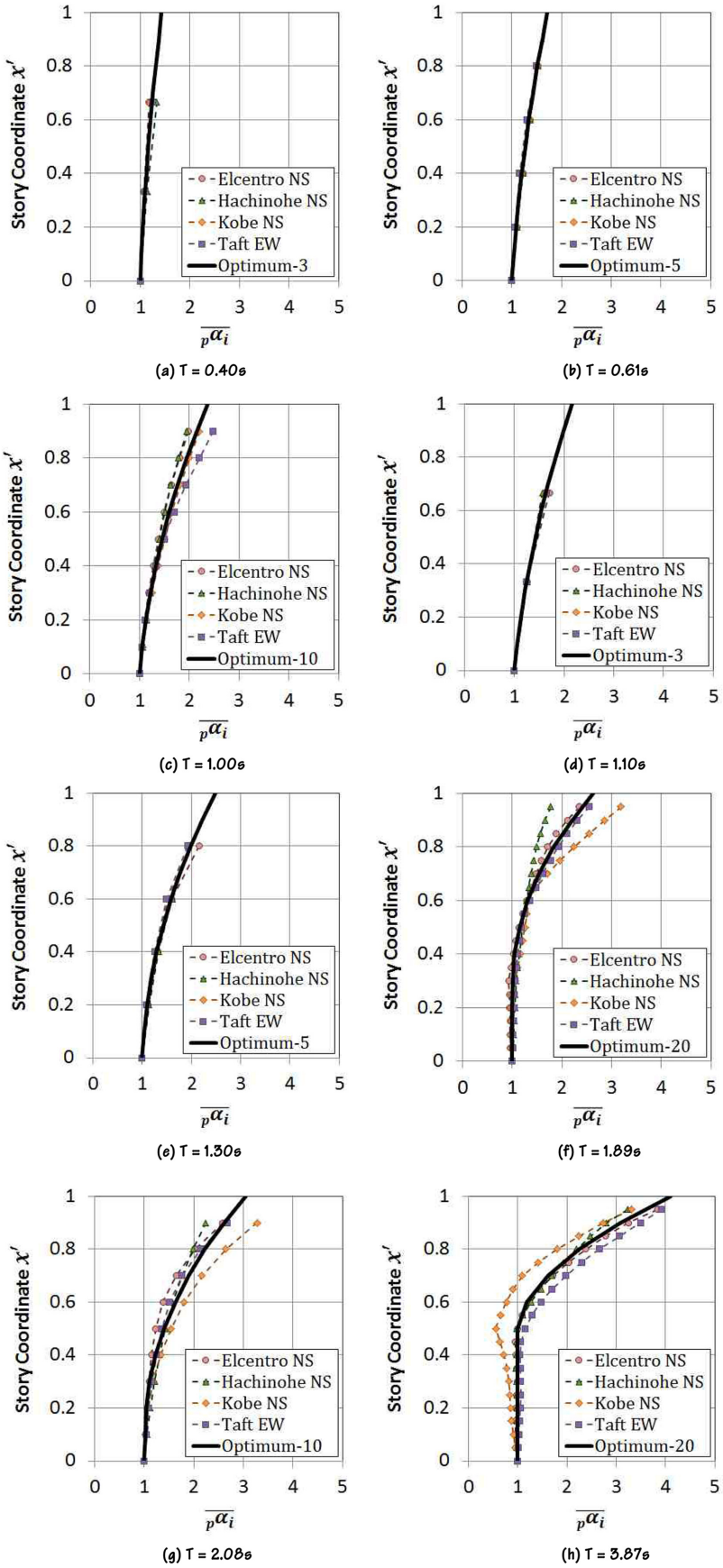


Figure 4-4. Generalized curve of optimum distribution of story shear force coefficient by natural vibration period.

Table 4-3. Variables of approximation formula of optimum distribution of story shear force coefficient

Natural vibration period	0.40s	0.61s	1.00s	1.10s	1.30s	1.89s	2.08s	3.87s
Variable A (Max. value)	0.43	0.71	1.37	1.16	1.49	2.04	1.63	3.10
Variable B (curvature)	1.37	1.43	1.64	1.46	1.85	2.33	3.11	4.31

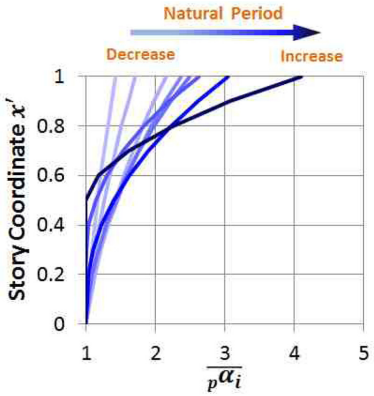


Figure 4-5. Pattern of optimum distribution of story shear force coefficient according to natural vibration period.

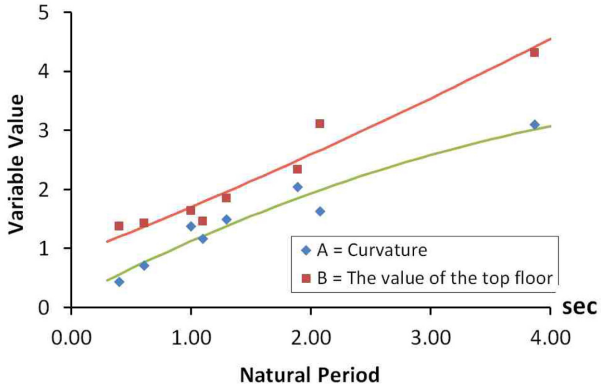


Figure 4-6. Variable distribution pattern of the proposed approximation formula.

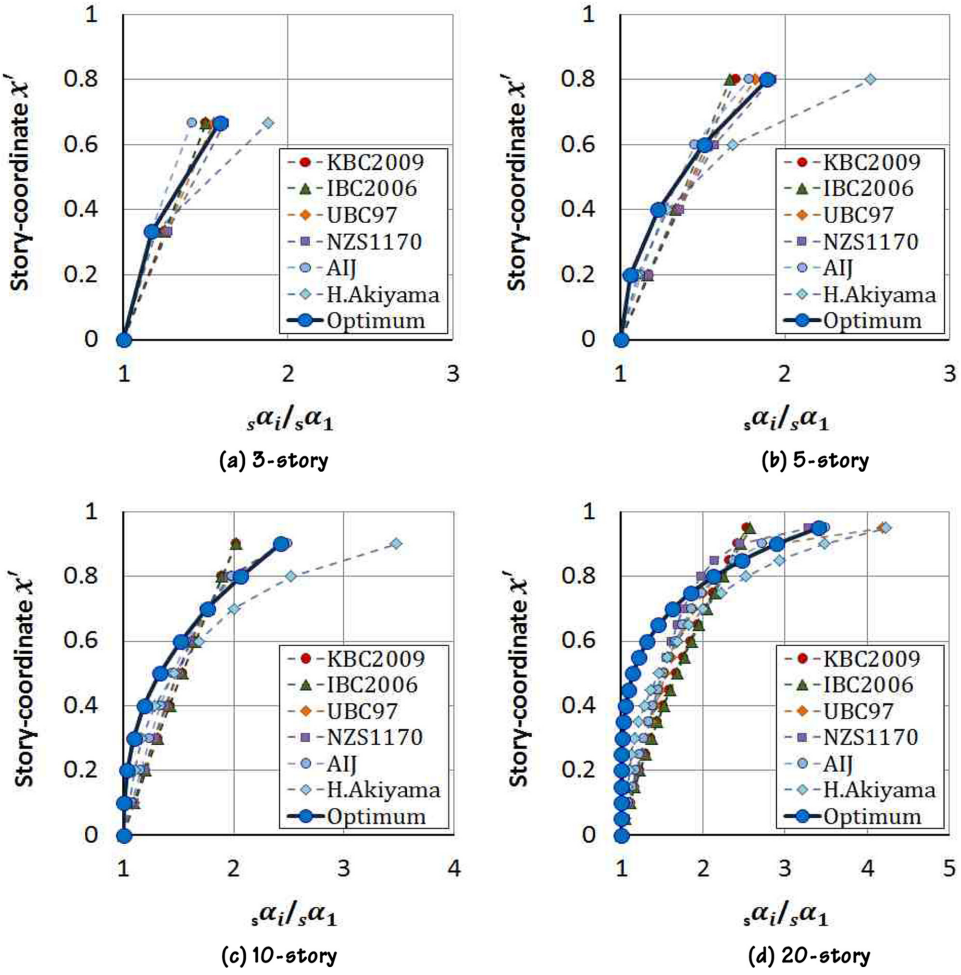


Figure 4-7. Optimum distribution of story shear force coefficient by the proposed calculation formula.

of story shear force coefficient described by the variable analysis according to the approximation formula in an exponential function form and the natural vibration period is as shown in Formula (4.4), and through this, the comparison between the graph of optimum distribution of story shear force coefficient estimated and that of story shear force coefficient based on the domestic and international seismic design code is as shown in Fig. 4-7.

$$\overline{{}_p\alpha_i} = 1 + \{A \times (x')^B\} \tag{4.4}$$

When, x' : Height up to the i story from the ground

$A = -0.08 \times T^2 + 1.05 \times T + 0.60$

$B = 0.03 \times T^2 + 0.80 \times T + 0.87$

T : Natural vibration period

4.3.2. Verification on the proposed calculation formula

The verification on the proposed calculation formula was conducted in the following manner: First, design a structure by applying the optimum distribution of story shear force coefficient in accordance with the distribution of story shear force coefficient, based on the seismic design code of several countries around the world, as well as the proposed calculation formula. Compare and analyze the layer damage distribution accordingly. We carried out the dynamic response analysis in the same way as described in Chapter 3, and estimated the distribution of cumulative plastic deformation ratio.

Although the distribution pattern of layer damage appeared in various forms, we calculated the average value for the layer damage distribution by the input earthquake motion in order to analyze the overall distribution pattern and displayed together in diagrams.

The pattern of layer damage distribution represented in average value showed a relatively stable form, except that over 50% of damages occurred on the 1st story in case of 3-story model expressing concern about the excessive damage concentration.

As for the analytical models in the same conditions though, comparing the layer damage distribution based on the proposed calculation formula and that of based on the seismic design code of several countries, the former showed the most evenly distributed layer damage among all analytical models.

The Figs. 4-8 and 4-9 show the comparison results of the layer damage distribution based on the proposed calculation formula to that of based on the domestic and

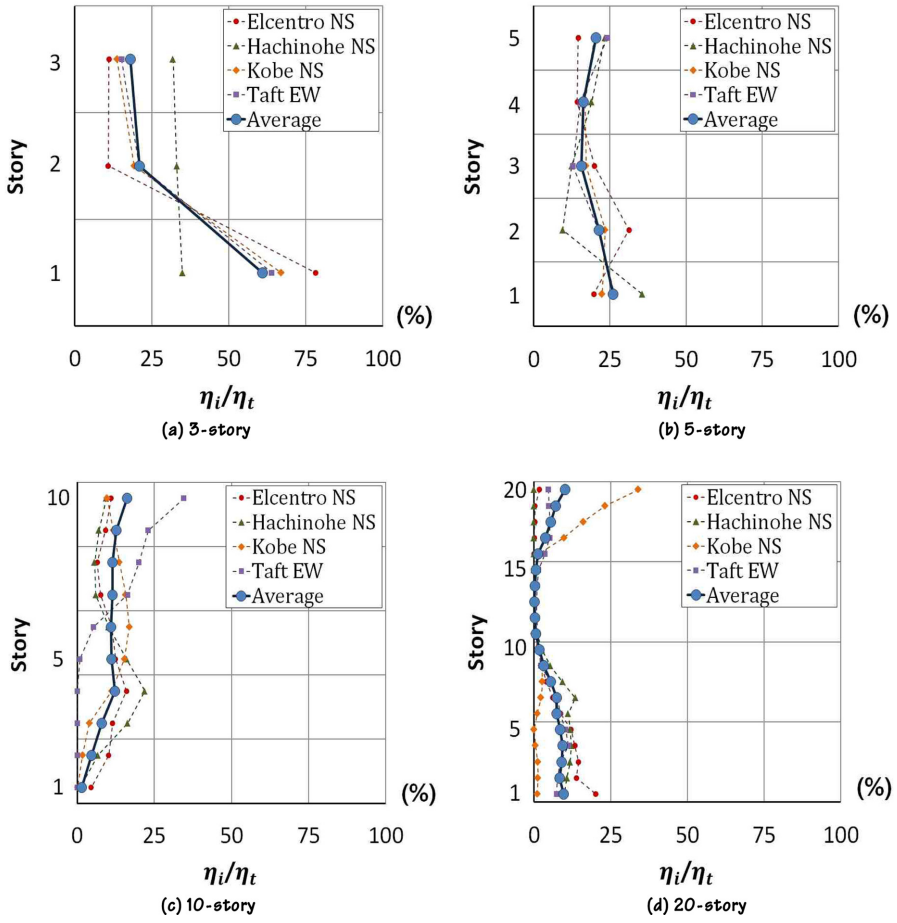


Figure 4-8. Cumulative plastic deformation ratio by the proposed calculation formula.

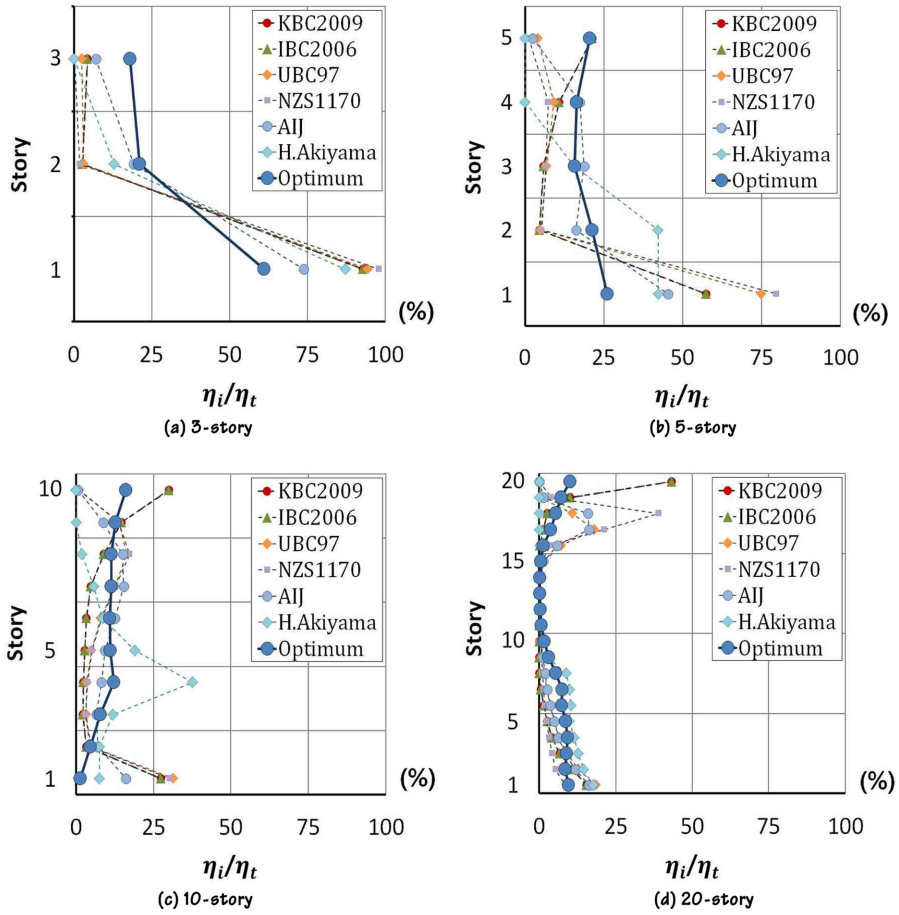


Figure 4-9. Verification of the proposed predict formula through comparison of cumulative plastic deformation ratio distribution.

international seismic design code respectively.

5. Conclusion

In this study, by using the story shear force design method based on the concepts of distribution of yield story shear force coefficients and cumulative plastic deformation ratio, we compared the characteristics of layer damage distribution based on the seismic design code of several countries around the world, and in conducting the response analysis of structures applied with these characteristics, analyzed the seismic efficiency such as the layer damage distribution and the energy absorbing capacity. In addition, we drew the optimum distribution of story shear force coefficient in diagrams, which uniformly distributed the layer damage to all stories, and proposed the calculation formula accordingly. The results thus obtained were as follows.

• Analysis on the distribution of story shear force coefficient based on the seismic design code of several countries around the world.

1) The distribution of story shear force coefficients based on KBC2009 and IBC2006 showed high in middle and lower portions compared to the other criteria, and low in linear fashion in upper portions.

2) The distribution of story shear force coefficients based on UBC97, NZS1170, AIJ and H. Akiyama showed a sharp increase in curvilinear form in top portion. The distribution increase in top portion was the most prominent in UBC97 and H. Akiyama criteria, and the distribution was low in lower portion of the H. Akiyama criterion forming the most modest.

• Analysis on response characteristics of a structure according to the distribution of story shear force coefficients

1) The response characteristics of a structure by static elasto-plastic analysis showed similar results, regardless of seismic design code, but those of a structure by dynamic response analysis showed a wide variety of forms, respectively.

2) In comparison of the distribution of cumulative plastic deformation ratios of analytical models according to a variety of input earthquake motions, the models KBC 2009 and IBC2006 with the linear type distribution of story shear force coefficients showed that the damage was tended to extremely concentrated in top portion.

3) The models UBC97, NZS1170, AIJ and H. Akiyama with the distribution of story shear force coefficients in curvilinear form showed that the layer damage was relatively well dispersed compared to the models KBC2009 and IBC2006. In analyzing the layer damage intensity and the energy absorption at limit state, the seismic efficiency of H.Akiyama model with the largest increase in distribution of story shear force coefficients in top portion was excellent.

• Proposal and verification on the calculation formula for optimum distribution of story shear force coefficients

1) We drew the optimum distribution of story shear force coefficients, implementing the optimum distribution of layer damage in which the damage distribution uniformly appears on all stories for analytical models having a variety of natural vibration periods, and proposed the calculation formula with variables resulted from analyzing the optimum distribution of story shear force according to the changes of natural vibration periods.

2) The layer damage distribution of analytical model applied with the proposed calculation formula of optimum distribution of story shear force coefficients showed a relatively uniform distribution, but the damage was somewhat concentrated in bottom portion of 3-story model.

3) With the analytical models in the same conditions, the layer damage distribution by the proposed calculation formula showed the most equitable form in comparison to the layer damage distribution obtained from the distribution of story shear force coefficients based on the seismic design code of several countries, and in case of the 3-story model which had some damage concentration, the layer damage distribution by the proposed calculation formula showed the most relaxed form.

However, the analytical models in this study have been simplified for the purpose of designing story-specific framework member and response analysis, so a study needed to be conducted in consideration of realistic member size, the collapse type of a structure, the behaviors of a structure due to the influence of gravity, etc. In addition, based on this study, the complementary measures on the proposed calculation formulas for optimum distribution of story shear force coefficients needed to be taken by expanding the scope of research on a wider range of aspect ratios and input earthquake motions, etc.

References

Akiyama Hiroshi, “Earthquake-Resistant Limit-State Design for Buildings”, Tokyo Univ. Press, 1985.

“KOREAN BUILDING CODE - STRUCTURAL”, Ministry of Construction & Transportation (Republic of Korea), 2009.

“International Building Code”, International Code Council (USA), 2006.

“Uniform Building Code”, International Conference of Building Officials (USA), 1997.

Architectural Institute of Japan, “AIJ recommendations for loads on buildings” (Japan), 1996/

Australia/New Zealand Standard 1170.4, New Zealand Standard (New Zealand), 2003.

“Study on the concept of performance-based seismic design and control of seismic response”, Ministry of Science and Technology (Republic of Korea), 2000.

J. S. Jeon, and S. H. Oh, “A Comparative Study on Story Damage Distribution of Domestic and Foreign Seismic Design Codes”, Busan Ulsan Gyeongnam Chapter of Architectural Institute of Korea - Workshop Presentation File, 8(1), pp. 126~129, 2012.

D. G. Lee, Y. W. Shin, and S. Y. Lee, “The Effect of Higher Vibration Modes on the Design Seismic Load”, Computational Structural Engineering Institute of Korea - Workshop Presentation File, pp. 73~78, 1990.

G. H. Park, D. G. Lee, and S. G. Lee, “Vertical Distribution of Seismic Loads for Multistory Building Structures”, *Journal of the Architectural Institute of Korea*, 7(5), pp. 239~250, 1991.

S. C. Jeong, and S. D. Kim, “Evaluation of the Story Seismic Load for Bearing Wall Type Structures”, Architectural Institute of Korea - Workshop Presentation File, 12(2), pp. 449~452, 1992.

K. J. Joo, and Y. W. Kim, “A Study on Distribution of Seismic Load for Dual System”, Architectural Institute of Korea - Workshop Presentation File, 13(1), pp. 279~282, 1993.

J. H. Park, “(A) Study on the Calculation of the Design Seismic Load Considering Dynamic Effect”, Dep. of Architectural Engineering Graduate school of Engineering, Kon-Kuk University, 1995.

J. H. Hwang, Y. S. Cheon, and L. H. Lee, “The vertical distribution of lateral seismic forces to account for the contribution of the higher modes”, *Journal of the Architectural Institute of Korea Structure & Construction*, 16(7), pp. 3-8, 2000.

G. H. Park, “A Study on the Vertical Distribution of Seismic Load for Equivalent Static Analysis of Shear Wall Type Building Structures”, *The Regional Association of Architectural Institute of Korea*, 7(2), pp. 69~77, 2005.

Y. B. Kim, H. K. Park, and D. H. Jeon, “Establishing Appropriate Seismic Force Distribution on Multistory Building Structures Subjected to Seismic Excitations”, *Journal of the Architectural Institute of Korea*, 10(12), pp. 219~224, 1994.

S. H. Oh, H. S. Yoo, and T. S. Moon, “Damage Distribution Rule of Weak Beam Type Multi-Story Steel Frames Influenced by Strength and Stiffness Ratios of Beam and Column”, *Journal of the Earthquake Engineering Society of Korea*, 9(5), pp. 53~61, 2005.

D. H. Jeon, and Inoue Yutaka, “On Optimum Distribution of Seismic Force Coefficients for Nonlinear High-rise Buildings Subjected to Earthquake Excitations”, Architectural Institute of Korea - Workshop Presentation File, 11(2), pp. 425~428, 1991.

S. H. Oh, Satoshi Yamada, and Hiroshi Akiyama, “Damage Distribution Rule of Weak Beam Type Multi-Story Steel Frames Influenced by Strength and Stiffness Ratios of

Beam and Cloumn", *AIJ*, No. 506, pp. 171~177, 1998.
Freeman, S., Sasaki, K., and Paret, T., "Multi-Mode Pushover Procedure (MMP) - A Method to Identify the Effects of Higher Modes in a Pushover Analysis", Proceedings of the 6th National Conference on Earthquake Engineering, EERI, Seattle, Washington, 1998.
Chopra, A. K, and Goel, R. K, "A modal pushover analysis procedure to estimate seismic demands for buildings: theory and preliminary evaluation", Pacific Earthquake Engineering Research Center, University of California, Berkeley, 2001.
Goman Ho, Peng Liu, and Michael Liu, "Parametric Analysis and Design Engine for Tall Building Structures", *International Journal of High-Rise Buildings*, 1(1), pp. 53~59, Korean Council on Tall Building and Urban Habitat (CTBUH), 2012.
D. H. Lee, T. J. Kim, J. H. Kim, and D. E. Kang, "State of Practice of Performance-Based Seismic Design in Korea", *International Journal of High-Rise Buildings*, 1(3), pp. 195~201, CTBUH, 2012.
Carl E. Grigorian and Mark Grigorian, "Drift Control for Multistory Moment Frames under Lateral Loading", *International Journal of High-Rise Buildings*, 2(4), pp. 355~365, CTBUH, 2013.